

Electronic supplementary information for Electrochemical setup — a unique chance to simultaneously control orbital energies and vibrational properties of single-molecule junc- tions with unprecedented efficiency

Ioan Bâldea ^{a‡}

S1 Method to Compute the Raman Spectra

The quantum chemical computations done to obtain the results obtained in this work will be briefly described below. In the experiments of Ref.¹ considered here, the viologen core is not directly contacted to (gold) electrodes in the molecular junctions used in experiment, but rather via alkyl linkers. Therefore, we did not include metal atoms in our quantum chemical calculations, but merely considered the isolated charged species of interest, namely dication (44BPY^{++}) and radical cation ($44\text{BPY}^{+\bullet}$). These charge species turned out to be essential for interpreting the transport experiments.¹ Focusing on these species allowed us to perform high-level quantum chemical calculations employing very good basis sets, namely, basis sets of triple-zeta quality augmented with diffuse functions (Dunning aug-cc-pVTZ).

Calculations for geometry optimizations and Raman spectra have been carried out at the DFT level by using the B3LYP hybrid exchange functional by means of GAUSSIAN 09.² The vibrational frequencies and the Raman intensities (activities in the language of GAUSSIAN 09²) computed for the two charge species (44BPY^{++} and $44\text{BPY}^{+\bullet}$) in acetonitrile are collected in Table S1, and Fig. 1, Fig. 2, Fig. S1, Fig. S2, Fig. S3, and Fig. S4. We specifically refer to acetonitrile as solvent because studies on bipyridine employed this solvent in experiments³ and because calculations using non-pure solvents¹ cannot be directly done with available program packages.² The data of Table S2 and S3 (computed for molecular species in benzene and vacuum, respectively) show no quantitative differences from those of Table S1 and emphasize that, for the effects considered in this paper, the nature of the environment is not critical; the essential role of the environment is to enable an efficient molecular orbital gating.

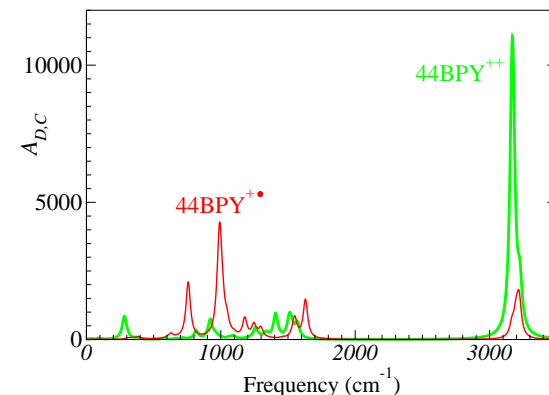


Fig. S1 Raman scattering activities of the dication 44BPY^{++} and cation $44\text{BPY}^{+\bullet}$ in acetonitrile. These spectra have been obtained by convoluting the computed spectral lines with Lorentzian functions of half-width 20 cm^{-1} .

S2 Method to Estimate the Charge of a Molecule in EC-STM Junctions from Transport Data

As a central point of the present analysis, we have used the transport data of Ref.¹ to show that the EC-STM transport setup does enable the switching between nearly perfect oxidized and reduced states.

The charge of a molecule embedded in a junction cannot be directly deduced from transport measurements. To determine the molecular charge (=LUMO occupancy n_l) and to demonstrate that, under electrochemical control, a continuous switching between an almost fully oxidized state ($n_l \approx 0$, 44BPY^{++}) and an almost fully reduced state ($n_l \approx 1$, $44\text{BPY}^{+\bullet}$), we have resorted to a model (namely, the Newns-Anderson model), which we have validated beforehand.

Originally proposed for chemisorption,⁴ the Newns-Anderson model was generalized to account for reorganization effects⁵ and further extended⁶ to studies on the adiabatic

^a Theoretische Chemie, Universität Heidelberg, Im Neuenheimer Feld 229, D-69120 Heidelberg, Germany.

[‡] E-mail: ioan.baldea@pci.uni-heidelberg.de. Also at National Institute for Lasers, Plasmas, and Radiation Physics, Institute of Space Sciences, Bucharest, Romania

No.	ω_D (cm ⁻¹)	ω_C (cm ⁻¹)	$\omega_D - \omega_C$ (cm ⁻¹)	A_D (Å ⁴ /a.m.u.)	A_C (Å ⁴ /a.m.u.)	$A_D - A_C$ (Å ⁴ /a.m.u.)
4	282.627	269.125	13.502	806.447	1.2534	805.193
5	291.38	309.634	-18.2538	21.9752	43.4161	-21.4409
6	291.761	343.131	-51.3703	21.8781	7.7725	14.1056
7	335.591	344.759	-9.1681	0.6434	37.1963	-36.5529
8	349.928	387.142	-37.2144	0.5949	81.8311	-81.2362
9	377.829	407.972	-30.1432	23.2752	5.9276	17.3476
10	378.109	535.73	-157.621	23.2231	2.416	20.8071
11	528.022	601.884	-73.862	2.7508	29.4361	-26.6853
12	574.551	603.499	-28.9471	19.3767	11.5002	7.8765
13	574.651	629.399	-54.7484	19.2539	156.018	-136.764
14	671.141	662.741	8.3996	22.4834	11.5542	10.9292
15	715.86	681.118	34.7414	21.0924	12.9927	8.0997
16	715.889	757.371	-41.4811	21.1223	2050.54	-2029.42
17	797.092	764.093	32.9987	2.2464	0.4111	1.8353
18	816.431	807.593	8.8375	145.846	2.5732	143.272
19	816.658	863.483	-46.8245	145.565	3.7531	141.812
20	921.545	891.828	29.7163	699.841	5.0171	694.823
21	945.94	961.739	-15.7985	2.1484	1.0493	1.0991
22	960.046	980.355	-20.3087	65.1111	728.289	-663.178
23	963.42	992.358	-28.9381	26.4929	3297.82	-3271.33
24	963.502	1002.38	-38.8772	26.6478	1.1897	25.4581
25	975.346	1011.99	-36.6487	16.198	678.864	-662.666
26	997.853	1020.71	-22.8578	27.8384	27.4713	0.3671
27	1010.6	1045.48	-34.8791	7.2104	446.243	-439.033
28	1062.33	1079.15	-16.8242	27.2854	14.7691	12.5163
29	1062.37	1097.9	-35.5331	27.2554	72.5765	-45.3211
30	1093.69	1110.4	-16.7031	101.919	11.6463	90.273
31	1113.77	1120.81	-7.036	4.6279	2.7734	1.8545
32	1202.57	1178.42	24.154	16.7542	697.476	-680.722
33	1214.74	1245.92	-31.1798	18.9443	460.854	-441.909
34	1258.47	1257.4	1.0701	404.255	2.9525	401.303
35	1297.54	1268.46	29.0808	19.4699	34.1741	-14.7042
36	1297.6	1298.07	-0.4722	19.4942	353.879	-334.385
37	1337.97	1313.59	24.3798	99.3676	0.1703	99.1973
38	1338.02	1353.76	-15.7331	99.3554	15.7712	83.5842
39	1408.16	1400.47	7.6865	447.486	4.3955	443.091
40	1408.22	1448.16	-39.9364	449.539	7.6421	441.897
41	1470.18	1463.03	7.1511	6.0276	24.1107	-18.0831
42	1509.69	1529.52	-19.8281	691.511	36.0463	655.465
43	1520.14	1549.78	-29.6319	0.9869	749.15	-748.163
44	1527.26	1580.71	-53.4499	328.644	4.3104	324.334
45	1569.24	1599.28	-30.0387	261.818	4.4524	257.365
46	1569.31	1629.73	-60.4191	261.012	1416.5	-1155.49
47	3165.11	3165.15	-0.0361	2011.03	246.87	1764.16
48	3165.14	3168.22	-3.076	2011.09	188.511	1822.58
49	3172.68	3192.41	-19.7328	6886.56	319.305	6567.26
50	3172.79	3198.73	-25.9371	293.968	168.294	125.674
51	3224.53	3201.58	22.9472	184.767	10.916	173.851
52	3224.6	3202.51	22.0845	184.536	385.805	-201.268
53	3225.24	3219.01	6.2369	241.682	3.166	238.516
54	3225.47	3220	5.4749	1002.42	1302.72	-300.302

Table S1 Vibrational frequencies (ω) and Raman activities (A) of the 44BPY dication (D) and cation (C) computed in acetonitrile at DFT/B3LYP/aug-cc-pVTZ level.

No.	ω_D (cm ⁻¹)	ω_C (cm ⁻¹)	$\omega_D - \omega_C$ (cm ⁻¹)	A_D (Å ⁴ /a.m.u.)	A_C (Å ⁴ /a.m.u.)	$A_D - A_C$ (Å ⁴ /a.m.u.)
4	243.511	233.684	9.8268	19.8079	0.1185	19.6894
5	282.597	274.896	7.7007	223.458	155.821	67.6373
6	331.497	302.044	29.4535	7.3262	430.212	-422.885
7	337.397	332.868	4.5286	0.0322	76.702	-76.6698
8	348.435	333.298	15.1362	22.5708	0.0113	22.5595
9	414.85	365.058	49.7929	6.746	0.54	6.206
10	421.748	372.722	49.0258	2.7798	22680.8	-22678
11	533.088	503.535	29.5534	1.071	0.6394	0.4316
12	535.394	629.802	-94.4084	0.8929	10.6579	-9.765
13	615.216	656.266	-41.05	2.3688	0.6279	1.7409
14	689.276	669.843	19.4332	5.8724	48792.3	-48786.5
15	712.94	678.537	34.4038	17.8453	0.0342	17.8111
16	717.854	701.722	16.1322	2.86	5.2526	-2.3926
17	801.374	716.888	84.4862	8.8168	0.8079	8.0089
18	817.497	786.933	30.5645	56.7959	1706.29	-1649.49
19	822.77	825.224	-2.4536	0.0399	0.4937	-0.4538
20	932.525	827.223	105.302	0.9719	114.3	-113.329
21	940.221	843.505	96.716	121.013	122.728	-1.7151
22	954.726	978.251	-23.5252	20.5983	19.4822	1.1161
23	960.026	984.411	-24.3847	112.309	38.3896	73.9191
24	971.324	990.091	-18.7669	0.4297	0.0131	0.4166
25	979.895	992.264	-12.3693	2.0291	1031.95	-1029.92
26	1005.33	1004.78	0.5445	4.0911	278.878	-274.787
27	1010.54	1038.66	-28.1261	5.5278	6.6733	-1.1455
28	1032.97	1093.11	-60.1452	0.0523	0.0282	0.0241
29	1074.31	1094.87	-20.5631	8.4554	8213.7	-8205.24
30	1081.16	1107.35	-26.1862	20.1834	0.0095	20.1739
31	1095.31	1111.62	-16.3067	2.5626	10.9727	-8.4101
32	1202.24	1210.76	-8.5138	16.0978	3.6235	12.4743
33	1211.06	1214.87	-3.8098	4.3724	10453.1	-10448.8
34	1238.21	1264.02	-25.813	137.71	371.208	-233.497
35	1263.25	1272.95	-9.7094	7.3245	2373.16	-2365.83
36	1284.42	1280.6	3.8199	26.2059	19838.6	-19812.4
37	1306.99	1325.86	-18.8693	35.1656	127.314	-92.1489
38	1334.82	1342.13	-7.3098	4.4126	2.3021	2.1105
39	1389.15	1392.71	-3.5672	59.0189	29.3272	29.6917
40	1428.74	1423.5	5.2454	116.403	0.0787	116.325
41	1478.45	1491.72	-13.273	0.6488	1.5614	-0.9126
42	1496.74	1511.66	-14.9178	161.448	5826.41	-5664.96
43	1510.21	1559.93	-49.722	22.9039	343.066	-320.162
44	1513.7	1560.62	-46.9197	0.2396	2.4364	-2.1968
45	1547.17	1575.29	-28.1269	11.3129	75560.5	-75549.2
46	1610.82	1589.92	20.9048	202.004	1510.36	-1308.36
47	3151.66	3169.4	-17.7455	1631.31	7346.16	-5714.85
48	3152.55	3170.22	-17.6695	84.6166	1213.13	-1128.52
49	3160.69	3174.53	-13.8425	7.7104	28.8476	-21.1372
50	3161.26	3176.08	-14.8244	2531.21	4739.7	-2208.48
51	3205.68	3205.42	0.2535	170.219	2750.46	-2580.24
52	3206.65	3205.77	0.8788	56.553	96.6258	-40.0728
53	3214.04	3211.19	2.8503	20.9338	469.309	-448.375
54	3215.12	3211.85	3.2615	459.872	5218.44	-4758.57

Table S2 Vibrational frequencies (ω) and Raman activities (A) of the 44BPY dication (D) and cation (C) computed in benzene at DFT/B3LYP/aug-cc-pVTZ level.

No.	ω_D (cm ⁻¹)	ω_C (cm ⁻¹)	$\omega_D - \omega_C$ (cm ⁻¹)	A_D (Å ⁴ /a.m.u.)	A_C (Å ⁴ /a.m.u.)	$A_D - A_C$ (Å ⁴ /a.m.u.)
4	234.688	278.358	-43.6699	7.2241	18.0921	-10.868
5	288.325	302.521	-14.1968	85.4626	12.4692	72.9934
6	332.408	335.831	-3.4234	0.102	0.175	-0.073
7	338.529	361.268	-22.7393	5.1528	0.0098	5.143
8	346.87	375.146	-28.2764	9.565	1249.2	-1239.64
9	396.074	390.139	5.9357	0.9528	25.576	-24.6232
10	420.384	505.852	-85.468	2.2002	0.2289	1.9713
11	529.806	507.621	22.1855	0.3927	0.0262	0.3665
12	545.151	633.945	-88.7938	0.5329	1.0332	-0.5003
13	610.771	654.896	-44.1252	0.9439	0.032	0.9119
14	688.549	689.557	-1.0082	5.4329	2938.31	-2932.88
15	706.934	697.707	9.2274	0.7564	0.0092	0.7472
16	711.882	703.797	8.0849	9.8028	0.3722	9.4306
17	796.663	718.22	78.4434	0.9811	1.0384	-0.0573
18	816.051	775.388	40.6637	19.7333	35.4116	-15.6783
19	838.246	827.266	10.98	0.0044	16.3007	-16.2963
20	919.877	846.169	73.7079	26.6515	41.5194	-14.8679
21	928.048	876.282	51.7662	0.4314	0.2178	0.2136
22	950.234	977.695	-27.4616	8.5455	5.6639	2.8816
23	960.091	981.915	-21.8239	58.097	11.0123	47.0847
24	965.284	987.913	-22.6297	0.5682	0.0064	0.5618
25	968.662	989.726	-21.0639	0.2029	66.6474	-66.4445
26	989.43	1006.01	-16.5761	1.0288	85.2251	-84.1963
27	1003.71	1038.29	-34.5852	3.4754	4.3021	-0.8267
28	1033.06	1093.18	-60.116	0.0011	827.379	-827.378
29	1069.88	1094.56	-24.6832	4.7984	0.0032	4.7952
30	1087.66	1105.62	-17.9577	12.791	0.0181	12.7729
31	1096.54	1111.12	-14.579	1.1309	0.8401	0.2908
32	1189.53	1211.96	-22.4293	7.8776	2.7269	5.1507
33	1203.77	1214.18	-10.4003	3.1656	764.513	-761.347
34	1236.52	1262.48	-25.9597	57.3397	95.2786	-37.9389
35	1267.05	1271.29	-4.2455	0.6088	516.049	-515.44
36	1274.22	1279.11	-4.8868	11.5287	1675.55	-1664.02
37	1303.37	1323.91	-20.5368	16.0595	26.8126	-10.7531
38	1328.84	1340.6	-11.7582	2.5379	2.3016	0.2363
39	1380.29	1393.3	-13.0057	19.2399	7.3816	11.8583
40	1424.21	1423.29	0.9173	36.0006	0.3457	35.6549
41	1476.49	1491.76	-15.2664	0.5298	0.9891	-0.4593
42	1485.95	1507.75	-21.797	39.3254	422.276	-382.951
43	1505.71	1566.75	-61.0438	7.1636	73.5392	-66.3756
44	1514.8	1573.56	-58.7601	0.0046	5764.19	-5764.18
45	1553.72	1576.19	-22.4729	4.5092	2.4217	2.0875
46	1610.45	1589.59	20.8626	73.4375	312.652	-239.215
47	3125.76	3165.64	-39.8825	833.146	1968.47	-1135.33
48	3126.56	3166.3	-39.7468	45.4571	379.865	-334.408
49	3135.58	3171.24	-35.6661	6.8499	20.6621	-13.8122
50	3136.45	3172.11	-35.6599	1186.51	1408.99	-222.484
51	3194.84	3201.3	-6.4614	56.5728	636.35	-579.777
52	3195.7	3201.77	-6.0667	34.4372	68.2005	-33.7633
53	3200.81	3204.6	-3.7855	8.2605	131.221	-122.961
54	3201.87	3205.36	-3.4871	231.031	887.583	-656.551

Table S3 Vibrational frequencies (ω) and Raman activities (A) of the 44BPY dication (D) and cation (C) computed in vacuum at DFT/B3LYP/aug-cc-pVTZ level.

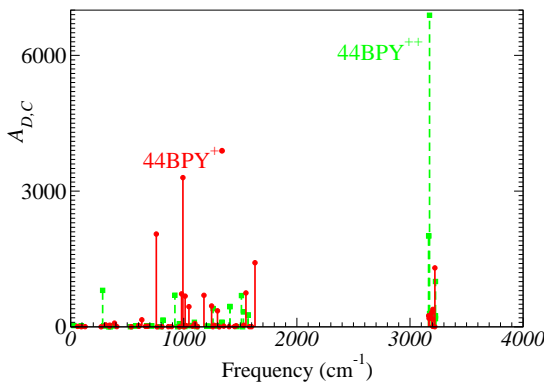


Fig. S2 Raman scattering activities (in $\text{\AA}^4/\text{a.m.u.}$) of the dicationic and cationic species in acetonitrile.

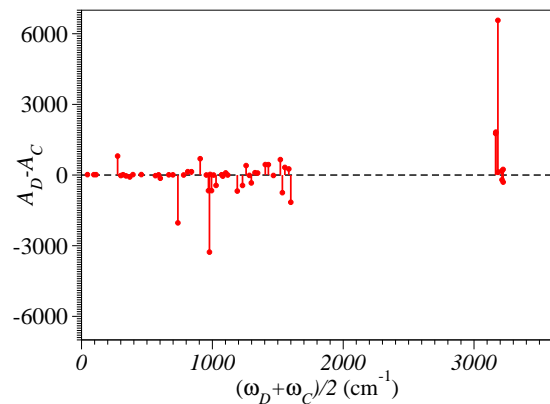


Fig. S4 Differences between the Raman scattering activities (in $\text{\AA}^4/\text{a.m.u.}$) of the dicationic and cationic species in acetonitrile plotted against the average frequencies $(\omega_D + \omega_C)/2$.

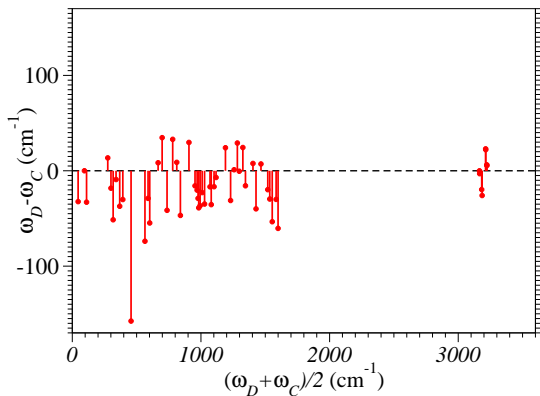


Fig. S3 Differences between the vibrational frequencies of the dicationic and cationic species in acetonitrile $\omega_D - \omega_C$ plotted against the average frequencies $(\omega_D + \omega_C)/2$.

transport through redox molecules. Recently,⁷ it was emphasized that this model is able to provide a robust description of the three-terminal transport through redox units.

The basic idea underlying the Newns-Anderson model is that the molecular transport is dominated by a single energy level. The experimental transport data¹ unambiguously indicated that the charge carriers are negative (n-type conduction). So, if there is a dominant molecular orbital (MO), it should be the lowest unoccupied molecular orbital (LUMO) of the dication 44BPY⁺⁺ ($n_l^D = 0$). The cation 44BPY^{+•} is described as

a fully reduced LUMO ($n_l^C = 1$).

To *microscopically* validate the idea that the LUMO should be the dominant MO, we have calculated the lowest electron affinities at the EOM-CCSD (equation-of-motion coupled cluster singles and doubles) level, which represents the quantum chemistry state-of-the-art for molecules of this size. These calculations, performed with CFOUR,⁸ showed that the difference between the first and second and higher electroaffinities (basically, the energies of LUMO and LUMO+1, LUMO+2, *etc* with reversed sign) are substantially larger than the LUMO offset relative to the metallic Fermi energy (as expressed by the small overpotential values of Fig. 4). This validates the transport description relying upon a single energy level, which is the basic idea of the Newns-Anderson model, within the realm of theory: the contribution coming from LUMO+1 (and higher unoccupied molecular orbitals) can be neglected.

The Newns-Anderson model allows one to compute the current $I = I(V_b, \eta)$ through an EC-STM junction as a function of the source-drain voltage $V_b = V_t - V_s$ and of the overpotential $\eta = V_{eq} - V_s$. All necessary formulas can be found in earlier work.^{6,7} Here we only briefly mention that the LUMO energy

$$\varepsilon_l = \lambda(1 - 2Q) - \xi e\eta - \gamma eV_b, \quad (\text{S1})$$

fluctuates due to reorganization effects described by an effective mode coordinate Q and the reorganization energy λ . The LUMO energy shift caused by the overpotential η and the source-drain bias V_b is characterized by the solvent gating efficiency ($0 < \xi < 1$) and the bias division factor ($0 < \gamma < 1$). In an EC-STM junction, finite level broadenings $\Gamma_{t,s}$ arise due to

couplings of the LUMO to the STM tip and substrate. The asymmetry of the molecule-electrode couplings $\delta \equiv \Gamma_t/\Gamma$, where $\Gamma \equiv (\Gamma_s + \Gamma_t)/2$, of the viologen-based EC-STM junctions is substantial albeit not so pronounced as recently found for azurin-based EC-STM junctions.⁷

We have used the Newns-Anderson model to fit the experimental currents measured in experiment¹ both in variable bias mode and constant bias modes. As visible in Fig. 3 and Fig. 4, the theoretical curves obtained within the Newns-Anderson model successfully reproduce the experimental currents¹ measured both in constant bias and variable bias modes.

Once the model has been validated against experiment¹ and the parameter values determined (they are indicated in the legends), the η - and V_b -dependent LUMO occupancy n_l (also shown in Fig. 3 and Fig. 4) has been determined using formulas reported earlier.^{6,7}

S3 Vibrational Frequencies and Raman Scattering Intensities of a Redox Molecule in a Biased Nanojunction

We have adopted a simple interpolation method to estimate the η - and V_b -dependent vibrational frequencies ω_v and Raman scattering intensities A_v of the various modes v . Namely, we have computed weighted averages of the dicationic (label D) and anionic (label C) species with appropriate weights (n_l and $1 - n_l$, respectively) expressed in terms of the LUMO occupancy n_l

$$\omega_v(\eta, V_b) = n_l(\eta, V_b)\omega_{v,D} + [1 - n_l(\eta, V_b)]\omega_{v,C}, \quad (\text{S2})$$

$$A_v(\eta, V_b) = n_l(\eta, V_b)A_{v,D} + [1 - n_l(\eta, V_b)]A_{v,C}. \quad (\text{S3})$$

The results expressing the dependencies of the vibrational frequencies and Raman scattering intensities on η and V_b are depicted in Fig. 5 and Fig. 6, respectively.

Besides modes 10 and 49 mentioned in the main text, we show in Fig. 5 and Fig. 6 the modes identified in Raman spectra of the radical anion $44\text{BPY}^{-\bullet}$ measured in acetonitrile:^{3,4} 4 (ring in-plane deformation; $6\text{a}^{3,9,10}$), 16 (ring breath; $1^{3,9,10}$); 23 (ring in-plane deformation; $12^{3,9,10}$), 27 (ring in-plane deformation; $18\text{a}^{3,9,10}$), 36 (CH in-plane bending; $9\text{a}^{3,9,10}$) and 46 (ring stretch; $8\text{a}^{3,9,10}$). Along with the present numbering in order of increasing frequencies (*cf.* S1), above we have given in parentheses the mode notation in use^{3,10} derived from benzene.⁹ The last mode (64 or 8a^9) is related to the so-called quinoidal distortion, corresponding to a shortening of the inter-ring C-C bond and of the C-C bond parallel to it, and a lengthening of the C-C bond between them as well as of the C-N bond.^{3,11}

Fig. S5 presents the dependencies of the integrated Raman spectrum $A_{tot}(\eta, V_b) \equiv \sum_v A(\eta, V_b)$. (Notice that signs of $V_b \rightarrow E_b$ and η of Ref.¹ are opposite to those employed here.)

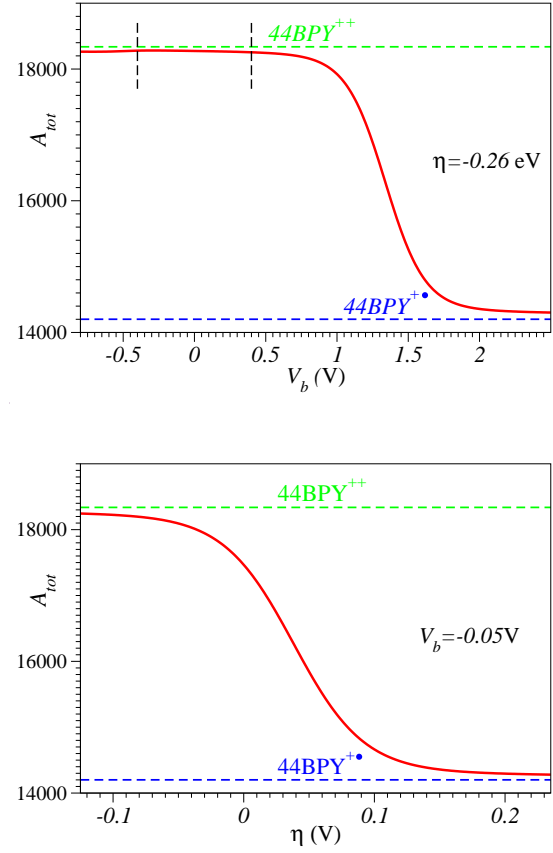


Fig. S5 Dependence on V_b and η of the integrated Raman scattering activity (in $\text{\AA}^4/\text{a.m.u.}$). The V_b -range sampled in experiment¹ is indicated by the two black vertical dashed lines.

Notes and references

- 1 I. V. Pobelov, Z. Li and T. Wandlowski, *J. Am. Chem. Soc.*, 2008, **130**, 16045– 16054.
- 2 M. J. Frisch, G. W. Trucks, H. B. Schlegel, G. E. Scuseria, M. A. Robb, J. R. Cheeseman, G. Scalmani, V. Barone, B. Mennucci, G. A. Petersson, H. Nakatsuji, M. Caricato, X. Li, H. P. Hratchian, A. F. Izmaylov, J. Bloino, G. Zheng, J. L. Sonnenberg, M. Hada, M. Ehara, K. Toyota, R. Fukuda, J. Hasegawa, M. Ishida, T. Nakajima, Y. Honda, O. Kitao, H. Nakai, T. Vreven, J. A. Montgomery, Jr., J. E. Peralta, F. Ogliaro, M. Bearpark, J. J. Heyd, E. Brothers, K. N. Kudin, V. N. Staroverov, T. Keith, R. Kobayashi, J. Normand, K. Raghavachari, A. Rendell, J. C. Burant, S. S. Iyengar, J. Tomasi, M. Cossi, N. Rega, J. M. Millam, M. Klene, J. E. Knox, J. B. Cross, V. Bakken, C. Adamo, J. Jaramillo, R. Gomperts, R. E. Stratmann, O. Yazyev, A. J. Austin, R. Cammi, C. Pomelli, J. W. Ochterski, R. L. Martin, K. Morokuma, V. G. Zakrzewski, G. A. Voth, P. Salvador, J. J. Dannenberg, S. Dapprich, A. D. Daniels, O. Farkas, J. B. Foresman, J. V. Ortiz, J. Cioslowski, and D. J. Fox, Gaussian, Inc., Wallingford CT, 2010 Gaussian 09, Revision B.01.
- 3 L. Ould-Moussa, O. Poizat, M. Castellà-Ventura, G. Buntinx and E. Kassab, *J. Phys. Chem.*, 1996, **100**, 2072–2082.
- 4 J. Muscat and D. Newns, *Progr. Surf. Sci.*, 1978, **9**, 1 – 43.
- 5 W. Schmickler, *J. Electroanal. Chem.*, 1986, **204**, 31 – 43.
- 6 I. G. Medvedev, *Phys. Rev. B*, 2007, **76**, 125312.
- 7 I. Bâldea, *J. Phys. Chem. C*, 2013, **117**, 25798–25804.
- 8 CFOUR, Coupled-Cluster techniques for Computational Chemistry, a quantum-chemical program package by J.F. Stanton, J. Gauss, M.E. Harding, P.G. Szalay with contributions from A.A. Auer, R.J. Bartlett, U. Benedikt, C. Berger, D.E. Bernholdt, Y.J. Bomble, L. Cheng, O. Christiansen, M. Heckert, O. Heun, C. Huber, T.-C. Jagau, D. Jonsson, J. Jusélius, K. Klein, W.J. Lauderdale, D.A. Matthews, T. Metzroth, L.A. Mück, D.P. O'Neill, D.R. Price, E. Prochnow, C. Puzzarini, K. Ruud, F. Schiffmann, W. Schwalbach, C. Simmons, S. Stopkowicz, A. Tajti, J. Vázquez, F. Wang, J.D. Watts and the integral packages MOLECULE (J. Almlöf and P.R. Taylor), PROPS (P.R. Taylor), ABACUS (T. Helgaker, H.J. Aa. Jensen, P. Jørgensen, and J. Olsen), and ECP routines by A. V. Mitin and C. van Wüllen. For the current version, see <http://www.cfour.de>.
- 9 G. Varsanyi, *Assignments for Vibrational Spectra of Benzene Derivatives*, Adam Hilger, London, 1974, vol. 1.
- 10 I. Bâldea, H. Köppel and W. Wenzel, *Phys. Chem. Chem. Phys.*, 2013, **15**, 1918–1928.
- 11 I. Bâldea, *Europhys. Lett.*, 2012, **99**, 47002.